JACS
JOURNAL OF THE AMERICAN CHEMICAL SOCIETY

Article

pubs.acs.org/JACS

Arylazopyrazoles as Light-Responsive Molecular Switches in Cyclodextrin-Based Supramolecular Systems

Lucas Stricker,[†] Eva-Corinna Fritz,[†] Martin Peterlechner,[‡] Nikos L. Doltsinis,[§] and Bart Jan Ravoo*[,†]

[†]Organic Chemistry Institute and Center for Soft Nanoscience, Westfälische Wilhelms-Universität Münster, Corrensstrasse 40, 48149 Münster, Germany

[‡]Institute of Materials Physics, Westfälische Wilhelms-Universität Münster, Wilhelm-Klemm-Strasse 10, 48149 Münster, Germany

[§]Institute for Solid State Theory and Center for Multiscale Theory & Computation, Westfälische Wilhelms-Universität Münster, Wilhelm-Klemm-Str. 10, 48149 Münster, Germany

Supporting Information

ABSTRACT: A simple and high yield synthesis of water-soluble arylazopyrazoles (AAPs) featuring superior photophysical properties is reported. The introduction of a carboxylic acid allows the diverse functionalization of AAPs. Based on structural modifications of the switching unit the photophysical properties of the AAPs could be tuned to obtain molecular switches with favorable photostationary states. Furthermore, AAPs form stable and light-responsive host−guest complexes with β-cyclodextrin (β-CD). Our most efficient AAP shows binding affinities comparable to azobenzenes, but more effective switching and higher thermal stability of the *Z*-isomer. As a proof-of-principle, we investigated two CD-based supramolecular systems, containing either cyclodextrin vesicles (CDVs) or cyclodextrin-functionalized gold nanoparticles (CDAuNPs), which revealed excellent reversible, light-responsive aggregation and dispersion behavior. To conclude, AAPs have great potential to be incorporated as molecular switches in highly demanding and multivalent photoresponsive systems.

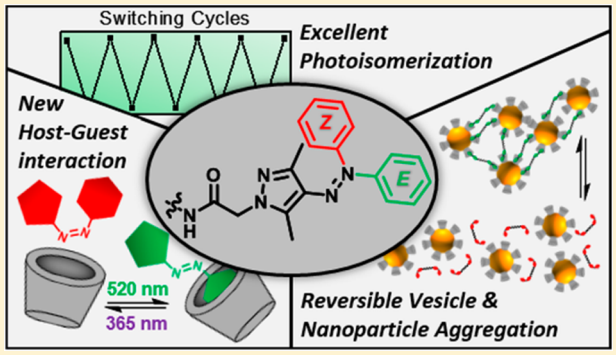

INTRODUCTION

Light-responsive molecular switches are widely used in different fields of chemistry due to the excellent spatial control of light exposure. One prominent example are azobenzenes which can be readily synthesized and modified, possess high quantum yields and extinction coefficients allowing reversible light-induced *E*/*Z*-isomerization over several cycles.[1] The photoisomerization and the resulting significant structural, chemical and physical changes of the thermodynamically stable *E*-isomer to the metastable *Z*-isomer were discovered in 1937 and have been extensively studied ever since.[2] Azobenzenes have been successfully applied for photocontrolled folding and unfolding of proteins and peptides,[3−5] as self-assembled monolayers (SAMs) on gold and silicon for reversible surface wettability or adsorption,[6−9] as light-responsive ligand for nanoparticles,[10−12] or for supramolecular materials that convert light into mechanical energy.[13,14]

Moreover, light-responsive host−guest complexes of α- or β-cyclodextrin (CD) with azobenzenes are known for a long time.[15] While the linear, nonpolar *E*-isomer forms an inclusion complex with α- and β-CD, the more polar and bent *Z*-isomer does not fit in either cavity. For that reason, diverse light-responsive supramolecular systems composed of azobenzenes and cyclodextrins were developed, for example, light-responsive hydrogels,[16−18] surfaces,[19,20] and drug delivery vehicles.[21] Combining such a light-responsive supramolecular system with gold nanoparticles[22] (AuNPs) allows one to address further fields of application due to their unique chemical and physical properties.[23−25] Particularly, when single AuNPs are densely packed, such as in supramolecular aggregates, new properties arise from the interparticular coupling of the surface plasmons which can be observed in the absorption spectrum.[26,27] Furthermore, our group reported on several examples of supramolecular systems composed of cyclodextrin vesicles (CDVs) self-assembled from amphiphilic cyclodextrins and azobenzenes as light-responsive molecular switches.[28−30]

Despite their extensive use as light-responsive switches, azobenzenes exhibit considerable disadvantages. For example, to trigger the $E \rightarrow Z$ isomerization, UV-light is necessary, which is harmful and can be massively scattered in biological tissue or in nanomaterials.[31−33] Additionally, the thermodynamic stability of the *Z*-isomer of most azobenzenes is low compared to other molecular switches such as diarylethenes.[34] As a result of the overlapping absorbances of both isomers, incomplete photoswitching is observed for azobenzenes. The photostationary state (PSS) for common azobenzenes is about 80% for the $E \rightarrow Z$ and 70% for the $Z \rightarrow E$ isomerization.[35] In

Received: January 14, 2016
Published: March 13, 2016

DOI: 10.1021/jacs.6b00484
J. Am. Chem. Soc. 2016, 138, 4547−4554

particular, in highly multivalent systems, this drawback can limit a complete switching since a large fraction of remaining *E*-isomer can still dominate the properties of the material.[35−37]

For that reason, a lot of research has been carried out to improve the azobenzene photoswitch. The development of azobenzenes that isomerize upon irradiation with visible light by varying the substitution patterns already resulted in impressive progress.[38] In this approach, the aim is either to shift the $\pi \rightarrow \pi^*$ band to longer wavelength or to obtain a splitting of the $n \rightarrow \pi^*$ band of the *E*- and *Z*-isomer, which usually overlap in the region of 400−500 nm.[39] Beside the first reported visible-light responsive azobenzene reported by Temps and co-workers[40] other important work has been published by the groups of Hecht[39,41] and Woolley.[42,43] They reported tetra-*o*-substituted azobenzenes, which showed splitting of the $n \rightarrow \pi^*$ band, resulting in good switching properties. *o*-Methoxy substituted azobenzenes were recently employed in a cyclodextrin-based hydrogel by Wang and co-workers.[18] Another approach that enhances the photoswitching and the thermal stability of the *Z*-isomer was reported by Fuchter and co-workers.[44] They introduced arylazopyrazoles as new light-responsive molecular switches. Substitution of one benzene by a pyrazole resulted in a significant red-shift of the $n \rightarrow \pi^*$ band of the *Z*-isomer, allowing nearly quantitative isomerization by irradiation with UV-($E \rightarrow Z$) or green light ($Z \rightarrow E$). Due to decreased steric repulsion within the *Z*-isomer arylazopyrazoles feature half-life times up to 1000 days. In general, heterocyclic azo-compounds are far less studied but offer a huge potential in the development of superior molecular switches.[44] Until now, most of the above-mentioned molecular switches are not suitable for CD-incorporated supramolecular systems, since they either bear no functional group for modifying the switching unit, are poorly water-soluble, undergo no host−guest complexation with CDs, or can be recognized in both isomeric forms.[45]

In this Article, we address these limitations and report water-soluble arylazopyrazoles (AAPs) that can be utilized in CD-based supramolecular systems featuring superior photoswitching characteristics compared to the standard azobenzenes (Figure 1). The synthesized AAPs showed excellent photophysical properties and selective host−guest complexation with CDs of the *E*-isomer, whereas the *Z*-isomer does not show any interactions. As a proof-of-principle, we successfully incorporated our AAPs in supramolecular systems of CDVs and CD-functionalized gold nanoparticles (CDAuNPs) and demonstrated the light-responsive aggregation and dispersion of these systems over several cycles.

EXPERIMENTAL SECTION

Materials. All chemicals used in this study were purchased from Alfa Aesar (Karlsruhe, Germany), Sigma-Aldrich Chemie (Taufkirchen, Germany), or TCI Europe (Zwijndrecht, Belgium) and used without further purification. β-CD was kindly donated by Wacker Chemie (Burghausen, Germany). Solvents were dried according to conventional methods before use.

Syntheses and Analyses. The syntheses of all compounds and CDAuNPs are described in the Supporting Information (SI). Moisture sensitive reactions were carried out in oven-dried glassware under inert atmosphere. Analytical thin layer chromatography was performed on Merck silica gel 60 F254 plates. Visualization of the compounds was achieved either under UV-light of 254 nm with a dual wavelength UV lamp (254 and 366 nm) (CAMAG, Muttenz, Switzerland) or by staining with basic permanganate solution. For column chromatography, silica gel 60 (230−400 mesh) was used. NMR spectra were recorded on a Bruker AV300 (300 MHz), Bruker AV400 (400 MHz), or Agilent DD2 (600 MHz) spectrometer. Chemical shifts were referenced to internal standards.

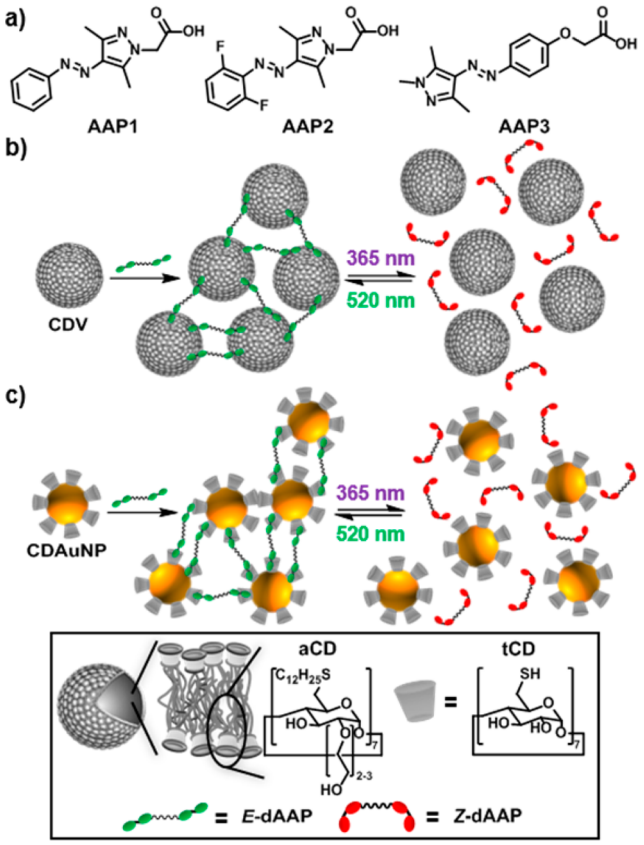

Figure 1. (a) Molecular structure of AAP1−3 and schematic representation of AAP- and CD-based supramolecular systems including (b) CDV and (c) CDAuNP.

Preparation of Cyclodextrin Vesicles (CDVs). The synthesis of amphiphilic cyclodextrin (aCD) and the preparation of unilamellar bilayer CDVs was carried out according to literature.[46] Several milligrams of aCD dissolved in a minimum amount of $CHCl_3$ was dried with a slight argon stream yielding a thin film in a small flask. Residual solvent was removed under high vacuum. Aqueous HEPES buffer (20 mM, pH = 7.2) was added to yield the desired concentration. After stirring overnight, the resulting suspension was repeatedly extruded for a minimum of 15 times through a polycarbonate membrane (diameter: 100 nm) in a Liposofast manual extruder.

Isothermal Titration Calorimetry (ITC). ITC was carried out using a TA Instruments Nano ITC Low Volume (Waters Corp., Milford, MA) with a cell volume of 170 μL using ITCRun version 2.1.7.0 Firmware version 1.31 (TA Instruments, WatersCorp., Milford, MA). All titrations were performed using a 50 μL syringe and 20 injections of 2.5 μL at a temperature of 25 °C with a stirring rate of 350 rpm while titrating the CD to the AAP solution. All samples were prepared in ddwater and degassed for 10 min before use. The data were analyzed using NanoAnalyse Data Analysis version 2.36 (TA Instruments, Waters Corp., Milford, MA), Microsoft Excel version 14.07113.5005 as part of Microsoft Office Professional Plus 2010 (Microsoft Corp., Redmond, WA) and OriginPro 9.1.G (OriginLab Corp., Northampton, MA). Before analysis, all data were corrected by subtraction of a blank titration of the CD into pure solvent.

UV/Vis Spectroscopy. UV/vis- and OD600 measurements were conducted using a JASCO V-650 double-beam spectrophotometer (JASCO Labor- and Datentechnik GmbH, Gross-Umstadt) at 25 °C using 1 mL low-volume disposable PMMA cuvettes (Brand GmbH & CO KG, Wertheim). The spectrometer was controlled by Spectra

DOI: 10.1021/jacs.6b00484
J. Am. Chem. Soc. 2016, 138, 4547−4554

Manager version 2.08.04 (Jasco Labor- and Datentechnik GmbH, Gross-Umstadt). The samples were dissolved in an appropriate solvent and measured against the same solvent. Data analysis was carried out using OriginPro 9.1G (OriginLab Corp., Northampton, MA). Optical density measurements were performed at λ = 600 nm where AAPs show no absorbance. Measurements were conducted for 60 min, and data points collected every minute. For all measurements, 1 mL of CDV (50 μM) dissolved in HEPES buffer (10 mM, pH = 7.2) was placed in a cuvette and measured. Addition of the desired amount of dAAP (2 mM stock solution in DMSO) occurred after 4 min. Spectra of the aggregation of CDAuNP were recorded in the range of 400−800 nm. Details about the concentration are described in the SI.

Dynamic Light Scattering (DLS). For DLS measurements a Malvern Nano-ZS instrument (Malvern Instruments) with low-volume disposable cuvettes kept at 25 °C was used. The average sizes of CDV, CDAuNP, and binary mixtures of AAPs with CDV or CDAuNP were measured after mixing the corresponding components.

Transmission Electron Microscopy (TEM). TEM investigations were performed using a Zeiss Libra 200FE with in-column energy filter (Carl Zeiss AG, Oberkochen, Germany) equipped with a Gatan US 4000 CCD camera (Gatan GmbH, München, Germany). For size measurements ImageJ 1.45s (National Institutes of Health, Bethesda, MD) was used. TEM samples were prepared by immersing the copper grid in the nanoparticle solution for 20 s. Grids were dried under ambient conditions overnight.

Photoswitching Experiments. Two different light sources were utilized for photoswitching experiments, a Rayonet photochemical reactor (The Southern New England Ultraviolet Company) equipped with 16 RPR-3500 lamps (365 nm) for $E \rightarrow Z$-isomerization and a LSC-G HighPower-LED emitting at 520 nm for $Z \rightarrow E$-isomerization.

RESULTS AND DISCUSSION

To obtain water-soluble and effectively photoswitchable AAPs that can undergo host−guest complexation, different structural modifications were investigated. By introducing a carboxylic acid group, AAPs can be easily further functionalized. To obtain an optimal photoisomerization three different structural modifications were designed and synthesized (Scheme 1). mAAP1 and mAAP3 differ in the position of the carboxylic acid group which should result in host−guest complexation occurring from the benzene side (mAAP1) or pyrazole side (mAAP3). In contrast to mAAP1, fluorine atoms were introduced at the *o*-positions of the benzene ring giving mAAP2. The synthesis of mAAP1−3 was performed according to a recently reported procedure in excellent yields (Scheme 1).[44] Starting from commercially available anilines diazo coupling with 2,4-pentadienone followed by condensation using either hydrazine or methyl hydrazine yielded AAPs. The carboxylic acid functionality was introduced via Williamson ether synthesis using methyl bromoacetate followed by ester hydrolysis giving AAP1−3. With regard to the light-responsive aggregation experiments AAP1−3 were functionalized either with a monovalent polyamine or a divalent amine yielding water-soluble mAAP1−3 or dAAP1−3, respectively. Details of the synthesis and analysis of all AAPs can be found in the SI.

UV/vis spectroscopy was carried out to investigate the photophysical properties of the prepared mAAPs. UV/vis spectra shown in Figure 2 clearly indicate the high potential of mAAP1−3 as molecular switches. Regarding the $E \rightarrow Z$-isomerization upon irradiation with UV-light (365 nm), all mAAPs show the characteristic changes in the absorbance which is a significant decrease and a slight blue-shift of the $\pi \rightarrow \pi^*$ band from 300 to 350 nm to ca. 300 nm and an increase of the $n \rightarrow \pi^*$ band around 430 nm. Additionally, a slight red-shift of the $n \rightarrow \pi^*$ band is observed for mAAP1 and mAAP3. Upon irradiation with green light (520 nm), the *E*-isomer is reformed.

Scheme 1. General Synthetic Strategy toward Water-Soluble Monovalent mAAP1-3 and Divalent dAAP1-3[a]

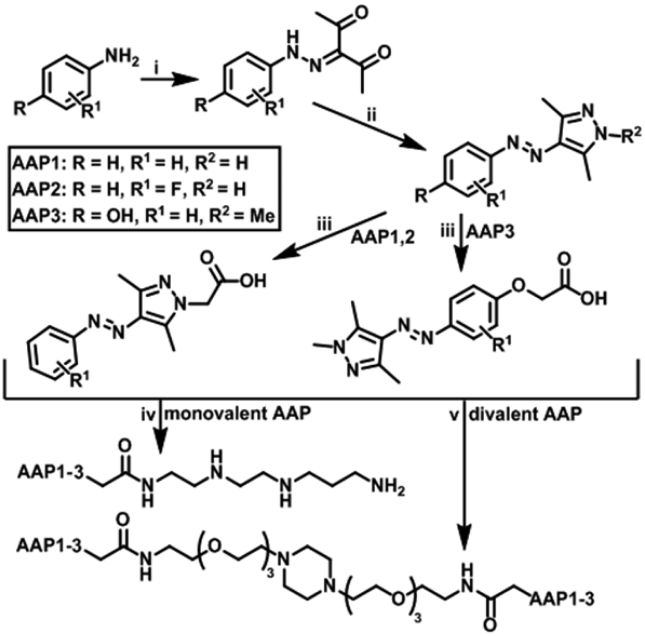

[a]Reaction conditions: (i) $NaNO_2$, HCl, AcOH, 2,4-pentadione, NaOAc, 85−90%; (ii) hydrazine × hydrate or methyl hydrazine, quant.; (iii) (1) methyl bromoacetate, K_2CO_3; (2) LiOH, 80−95%; (iv) (1) Boc-protected polyamine, PyBOP, DIPEA, 98−100%; (2) acetyl chloride, quant.; (v) divalent amine linker, EDCl, HOBt, NMM, 67−74%.

Remarkably, the reobtained intensity of mAAP1 and mAAP3 amounts to 94% which is almost quantitative. However, mAAP2 only returns to 71% of the initial intensity. The efficient photoisomerization of mAAP1 and mAAP3 can be explained by the observed red-shift of the $n \rightarrow \pi^*$ bands for the *Z*-isomers resulting in higher extinction coefficients at wavelengths above 500 nm and the consequent splitting of the $n \rightarrow \pi^*$ absorbances for the *Z*- and *E*-isomers of mAAP1 and mAAP3 which allows a more specific excitation. For mAAP2, no red-shift of the $n \rightarrow \pi^*$ absorbance is observed resulting in a lower switching efficiency (see insets in Figure 2). Calculated spectra of all AAPs ($CONH_2$-terminated) were obtained by time-dependent density functional theory (TDDFT), revealing good agreement with the measured spectra. In general a slight red-shift of the absorbances are observed for the calculated spectra (Figure 2, dashed curves).

The PSSs of mAAP1−3 rating the efficiency of the photoisomerization were determined by ^{1}H NMR spectroscopy (Figure 3). To this end, NMR spectra of the *E*-, *Z*-, and reformed *E*-isomer of mAAP1−3 were recorded directly after irradiating for 60 min. Exemplarily for all mAAPs, the aromatic region of the NMR spectra of mAAP1 is shown in Figure 3 (full spectra of mAAP1−3 can be found in the SI). Comparing the spectra of the *E*- and the *Z*-isomer, the signals for the *E*-isomer almost vanished completely whereas three new signals of the *Z*-isomer arose shifted to lower fields. Upon the second irradiation with green light, the initial signals of the *E*-isomer reappeared, whereas the signals of the *Z*-isomer disappeared. Based on signal integration, the PSS of mAAP1 amounts to ca. 90% for both isomerization processes. The PSS of mAAP2 and mAAP3 as well as the corresponding half-life times are listed in Table 1 supporting the UV/vis spectroscopic findings. Details

DOI: 10.1021/jacs.6b00484
J. Am. Chem. Soc. 2016, 138, 4547−4554

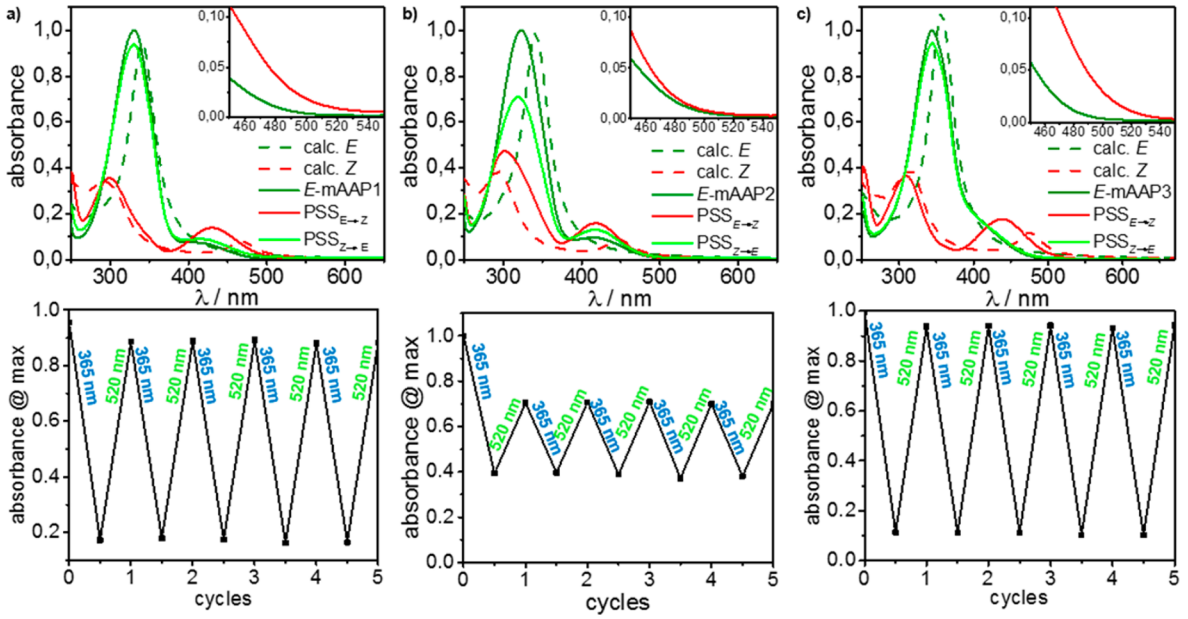

Figure 2. Experimental normalized and calculated UV/vis spectra of the photoisomerization of mAAP1−3 in water: (a) mAAP1, (b) mAAP2, and (c) mAAP3 (each 50 μM; irradiation time 10 min). Insets: zoom-in at the 500 nm area.

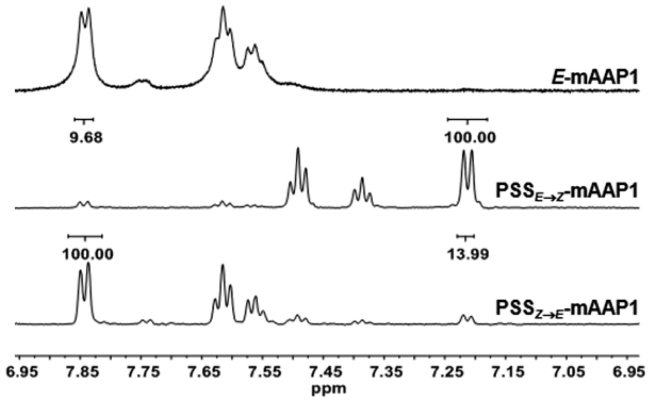

Figure 3. Aromatic region of the ^{1}H NMR spectra of the *E*-isomer, $PSS_{E\rightarrow Z}$, and $PSS_{Z\rightarrow E}$ of mAAP1 recorded in D_2O (0.5 mM; irradiation time 60 min).

Table 1. Summary of Photophysical Properties of AAP1-3 in Comparison to Azobenzene

	$PSS_{E\rightarrow Z}$	$PSS_{Z\rightarrow E}$	$\tau_{1/2}$ *Z*-state
azobenzene	80%[35]	70%[35]	5.70 days
mAAP1	92%	88%	9.49 days
mAAP2	94%	55%	≫11 days
mAAP3	89%	92%	1.32 days

about the determination of the half-life time can be found in the SI.

In summary, the photophysical properties clearly indicate that AAPs are highly interesting candidates as molecular switches. mAAP1 and mAAP3 showed excellent light-responsive isomerization behavior which is superior to the light-response of commonly used azobenzenes. Therefore, our data is in good agreement to the work of Fuchter and co-workers demonstrating quantitative isomerization for AAPs.[44] Regarding our structural modifications, the functionalization of AAPs with carboxylic acid groups resulted only in a marginal decrease of the PSS. However, the introduction of the *o*-F substituents increases the half-life time of the *Z*-isomer of mAAP2. Similar observations have been reported by Hecht and co-workers. The efficiency of the $E \rightarrow Z$-isomerization remains unchanged, whereas the PSS of the $Z \rightarrow E$-isomerization drops drastically to 55% due to the complete overlap of the $n \rightarrow \pi^*$ bands of both isomers. It follows that mAAP1 features the best photophysical properties and AAP1 should be a promising molecular switch for applications in multivalent host−guest systems. Additionally, the quantum yields for the photoisomerizations of all AAPs were determined by irradiation time dependent UV/vis measurements. The calculated quantum yields can be found in the SI.

The optimized geometry of all AAPs (terminated by $CONH_2$) were calculated by the DFT method. In all predicted structures, the *E*-isomers show a planar structure, whereas the *Z*-isomers adopt a twisted geometry to minimize the steric strain between the methyl groups of the pyrazole ring and the phenyl ring (Figure 4 and Figure S9). These results are similar

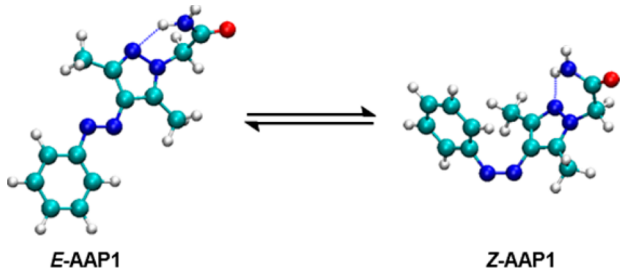

Figure 4. DFT-optimized geometry of *E*/*Z*-AAP1 terminated with $CONH_2$.

to the geometries calculated by Fuchter and co-workers.[44] The summarized calculated changes in relative energy and the rotation barrier of AAPs are stated in the SI.

Next, we investigated if *E*-mAAP1−3 can form host−guest complexes with α-and β-CD. To this end, isothermal titration calorimetry (ITC) was carried out to determine the binding constants of each interaction. ITC results of each titration is

DOI: 10.1021/jacs.6b00484
J. Am. Chem. Soc. 2016, 138, 4547−4554

summarized in Table 2 (corresponding titration curves can be found in the SI). As comparison, *E*-azobenzene with a

Table 2. Binding Constants of α-CD and β-CD with *E*-AAPs and *E*-Azobenzene Determined via ITC

guest	host	K ($\times 10^2$ M^{-1})
E-azobenzene[35]	α-CD	59.0
E-azobenzene[35]	β-CD	24.0
E-mAAP1	α-CD	4.01
E-mAAP1	β-CD	23.8
E-mAAP2	α-CD	
E-mAAP2	β-CD	5.05
E-mAAP3	α-CD	
E-mAAP3	β-CD	18.3
E-dAAP1*	β-CD	35.9
E-dAAP3	β-CD	

comparable substituent shows 1:1 interactions with α- and β-CD with binding constants of $K \sim 10^3$ M^{-1}.[35] All three *E*-isomers form stable 1:1 host–guest inclusion complexes with β-CD. In the case of *E*-mAAP3, an interaction of $K = 18.3 \times 10^2$ M^{-1} was quite unexpected due to the fact that the pyrazole unit is similar to an imidazole which is not a suitable guest because of its high polarity.[47] Therefore, we assume that binding occurs via the substituted benzene unit, resulting in a threading-like complexation placing the benzene unit in the CD cavity. In contrast, the benzene unit is easily accessible for mAAP1 and mAAP2 and can be placed inside the cavity without threading (Figure 5c). ITC measurements of *E*-dAAP3 confirmed our

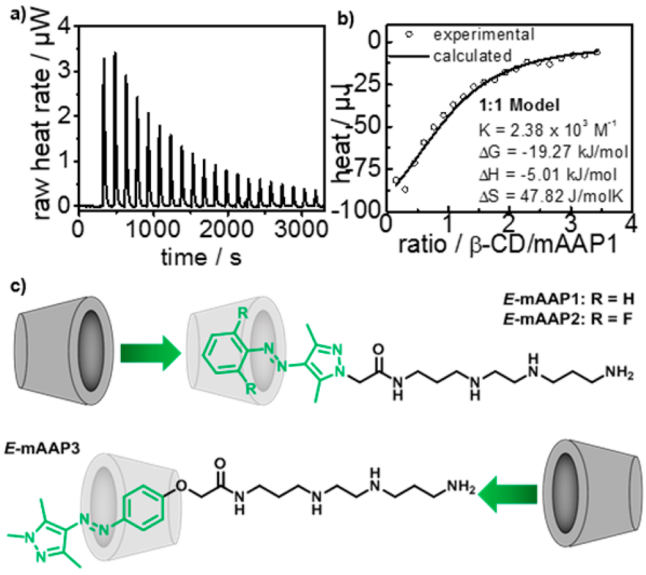

Figure 5. (a) ITC titration curve. (b) Corresponding 1:1 fit of *E*-mAAP1 and β-CD (*E*-mAAP 1 mM and β-CD 10 mM in H_2O). (c) Proposed binding mechanism for mAAP1–3.

hypothesis concerning the binding mechanism since no interaction of *E*-dAAP3 with β-CD can be detected (Figure S10). In the dimer, both ends of the molecule are blocked by the bulky methylated pyrazole prohibiting the threading. As a consequence there is no possibility to place the benzene inside the CD cavity. *E*-mAAP2 revealed a rather low binding constant of $K = 5.05 \times 10^2$ M^{-1} which can be explained by the fact that in general fluorinated aromatic compounds show less affinity to CDs.[48] The highest binding constant is found for the inclusion complex of β-CD and *E*-mAAP1 which amounts to $K = 23.8 \times 10^2$ M^{-1} and is comparable to the interaction between β-CD and azobenzene (Figure 5). Regarding α-CD, ITC titrations reveal that the smaller sized CD shows only a weak interaction with *E*-mAAP1. No significant host–guest complexation was detected with *E*-mAAP2 and *E*-mAAP3. For the determination of the binding constant of the dimer of AAP1, we used dAAP1*, in which the AAP units are linked by a polyamine instead of a tetraethylene glycol chain. dAAP1* has significantly higher water solubility than dAAP1. In earlier work, our group has already shown that also these dimers are suitable cross-linkers for CDV.[49] In further experiments, we only used dAAP1 for cross-linking of CDV or CDAuNP to avoid electrostatic interactions of the polyamine linker with the negative surface of AuNPs.

Based on our preliminary results and with regard to the incorporation of AAPs into CD-based supramolecular systems, we focused on investigations of β-CD as host molecule. As guest molecules, we used the divalent dAAP1–3. The construction of such supramolecular systems shall be a proof-of-principle demonstrating the versatility of AAPs as photoswitches. First, we developed a supramolecular system of dAAP1–3 and cyclodextrin vesicles (CDVs). CDVs are unilamellar bilayer vesicles composed of amphiphilic CD with a size of ca. 100 nm. These nanostructures combine the characteristics of vesicles and cyclodextrins and display β-CD cavities at the vesicle surface.[46] To characterize the formation of the host–guest inclusion complexes time-dependent optical density measurements at 600 nm (OD600) were performed (Figure 5a). Hereafter, the characterization is exemplarily discussed for dAAP1, the results of dAAP2–3 can be found in the SI. At $t = 0$ min, CDVs show an OD600 of 0.049 which increases immediately upon the addition of *E*-dAAP1 and reaches a plateau after 60 min. The extent of the increasing OD600 depends on the guest concentration which is due to the noncovalent cross-linking of the CDVs by the divalent guest and the resulting vesicle aggregation. Both control experiments, the addition of *Z*-dAAP1 to CDVs and *E*-dAAP1 measured in the absence of CDV, did not affect the optical density. Furthermore, the size of the formed aggregates was determined by dynamic light scattering (DLS). Upon addition of 10 μM *E*-dAAP1 to CDVs, the average size of the aggregates changes from 120 to 2200 nm, whereas no significant change was observed when the corresponding *Z*-isomer was added (Figure 6b). The reversible, light-responsive aggregation and dispersion of this supramolecular system upon alternating light irradiation was again followed by DLS and OD600 (Figure 6c). The applied concentration of *E*-dAAP1 was 10 μM. Starting from the vesicle aggregates, irradiation with UV-light results in a decrease in the OD600 to 0.07 and of the hydrodynamic diameter to 136 nm. Upon second irradiation with green light the OD600 value increased to 0.65 and the hydrodynamic diameter to 2500 nm. In total, the light-induced switching between the aggregated and dispersed state was possible over at least five cycles without decreasing efficiency. These findings demonstrate the highly reversible and light-responsive character of the AAP/CD-based supramolecular system.

In comparison, the divalent fluorinated guest *E*-dAAP2 is indeed able to induce the aggregation of CDVs although a much higher guest concentration is necessary to achieve the same increase in OD600 compared to *E*-dAAP1 (Figure S17). To obtain an OD600 of 0.3, a 5-fold higher concentration of 30

DOI: 10.1021/jacs.6b00484
J. Am. Chem. Soc. 2016, 138, 4547–4554

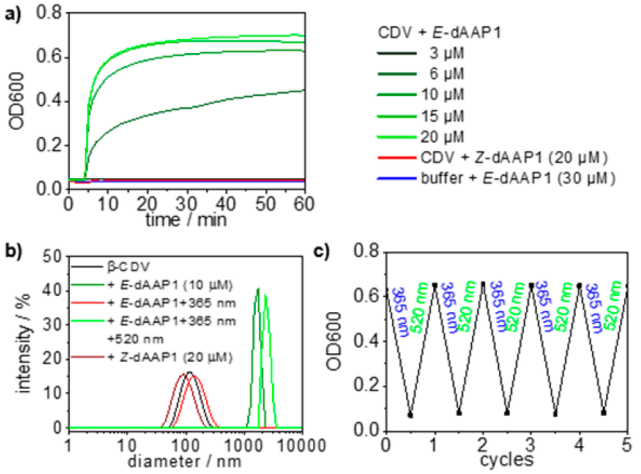

Figure 6. (a) OD600 of concentration-dependent aggregation of CDV and *E*-dAAP1 and reversible aggregation and dispersion of CDV and dAAP1 studied by (b) DLS and (c) OD600 (*E*-dAAP1 10 μM, *Z*-dAAP1 20 μM, aCD 50 μM, irradiation time 10 min).

μM had to be added. The corresponding DLS measurements showed the expected signal at 1200 nm but also a second signal indicating remaining nonaggregated vesicles (Figure S17). An explanation for these results might be the lower binding affinity of *E*-mAAP2 to β-CD (see Table 2). Nevertheless, a UV-light-induced dispersion of the aggregated CDVs could be observed whereby OD600 and DLS values of 0.08 and 140 nm are comparable to the results of *E*-dAAP1. A significant reaggregation upon a second irradiation with green light cannot be observed which is likely due to the combination of the incomplete photoswitching (PSS of 55%) and the rather low binding constant (K = 505 M^{-1}) of *E*-mAAP2. Longer irradiation times of 60 min only result in an increase to 0.12 in the OD600, aggregates could not be detected by DLS. A second cycle of photoswitching revealed no significant difference between the *E*- and *Z*-isomer. We conclude that dAAP2 is an inferior molecular switch compared to dAAP1.

The addition of *E*-dAAP3 as a guest molecule resulted in no aggregation of CDVs (Figure S18). These findings support the proposed host–guest complexation of β-CD being threaded from the polyamine end to the benzene for the monomeric guest (*E*-mAAP3) which is not possible for the divalent structure. We conclude that dAAP3 is not a suitable divalent cross-linker for CDVs.

Based on the results of the *E*-dAAP-induced aggregation of CDVs which clearly show that dAAP1 is the most efficient light-responsive guest, we focused on this guest molecule for the incorporation in the second proof-of-principle supramolecular system based on CDAuNPs. First, water-soluble CDAuNPs were synthesized by reducing Au^{3+} in the presence of perthiolated β-cyclodextrin (tCD). The successful immobilization of tCD on the AuNPs can be observed from the ^{1}H NMR spectra showing characteristic signals for tCD that are significantly broadened compared to the unbound ligand (NMR spectra and further characterization of CDAuNPs can be found in the SI). To investigate the host–guest complexation of CDAuNPs and *E*-dAAP1 and the resulting aggregation-induced plasmon coupling, UV/vis spectroscopy was carried out (Figure 7a). To this end, different concentrations of *E*-dAAP1 (0–0.25 mM) were added to CDAuNPs and allowed to equilibrate for 2 h. The resulting spectra show a red-shift and

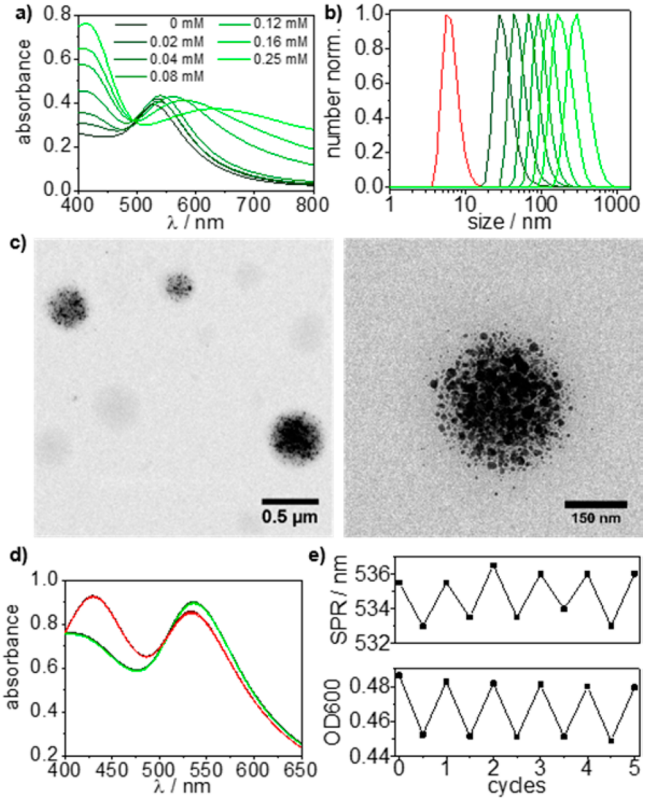

Figure 7. Investigations of the concentration-dependent aggregation of CDAuNP and *E*-dAAP1 by (a) UV/vis spectroscopy, (b) DLS (*E*-dAAP1 0.08–0.25 mM (green gradient), *Z*-dAAP1 0.16 mM (red curve)), and (c) TEM (0.16 mM); the reversible aggregation and dispersion of CDAuNP and dAAP1 monitored by (d) UV/vis spectroscopy; (e) the SPR band (top) and the OD600 value (bottom) (*E*-dAAP1 0.16 mM, CDAuNP 0.05 mg, irradiation time 3 min (520 nm) and 10 min (365 nm)).

broadening of the SPR band which is more pronounced with increasing *E*-dAAP1 concentration indicating the expected particle aggregation. Exemplarily, an *E*-dAAP1 concentration of 0.25 mM results in the significant shift from 529 nm (0 mM) to 628 nm. DLS measurements confirm that increasing concentrations of *E*-dAAP1 can be correlated to an increasing size of the formed aggregates (Figure 7b). Furthermore, it is possible to control and adjust the size of the aggregates in the range of ca. 30 and 300 nm. As a control experiment, *Z*-dAAP1 (0.16 mM) was added which did not result in an aggregation of CDAuNPs (Figure 7b) or a shift in the SPR band (Figure S21).

Transmission electron microscopy (TEM) was carried out to obtain further information on the shape and the macroscopic structure of the CDAuNP aggregates. TEM samples were taken from highly diluted aggregate solution to prevent aggregation effects simply caused by the drying of the TEM grid. In Figure 7c, aggregates induced by an *E*-dAAP1 concentration of 0.16 mM are shown. Remarkably, all imaged CDAuNPs are clustered in aggregates. CDAuNPs are aggregated in a high density which is increasing in a radial fashion toward the center of the aggregates indicating a spherical shape. The light-responsive and reversible aggregation and dispersion upon alternating light irradiation was investigated by the position of the SPR band as well as the OD600. First, CDAuNP aggregates using an *E*-dAAP1 concentration of 0.16 mM were formed upon irradiating with green light for 3 min (Figure 7d, green gradients). The SPR band is located at 536 nm and the OD600

DOI: 10.1021/jacs.6b00484
J. Am. Chem. Soc. 2016, 138, 4547–4554

value amounts to 0.49. Focusing on the n → π* band around 430 nm of dAAP1, the isomerization to *Z*-dAAP1 within the CDAuNP aggregates is completed after irradiating with UV-light for 3 min (Figure 7d, red gradients). More interestingly, the position of the SPR band is blue-shifted to 533 nm and the intensity at 600 nm is decreased to 0.45, both strongly indicating a dispersion of the aggregates. Upon irradiating the dispersed sample again with green light, reaggregation can be observed since both the position of the SPR band as well as the OD600 value are recovered (Figure 7e). Altogether, the light-responsive switching between the aggregated and dispersed state is fully reversible over five cycles.

CONCLUSION

In summary, we have presented water-soluble AAPs and their huge potential as efficient molecular switches in a variety of CD-based supramolecular systems. Our key structural modification of the AAP unit is the introduction of a carboxylic acid group which can be easily further functionalized. The synthesis of the mono- and divalent AAPs is straightforward and proceeds in high yields, and the final compounds have excellent water solubility. Comparing mAAP1−3, we showed how structural modifications of the switching unit affect the photophysical properties. All monovalent mAAPs showed excellent *E* → *Z*-isomerization and favorable photostationary states. mAAP1 features the most attractive photophysical properties and forms a stable and light-responsive 1:1 host−guest complexation with β-CD. Light-responsive switching of this inclusion complex is more efficient and the thermal half-life time of the *Z*-isomer is superior compared to commonly used azobenzenes. On the basis of two examples of CD-based supramolecular systems, we demonstrated the diversity of possible applications of AAPs as molecular switches. Both the incorporation of dAAPs in a system containing CDVs and CDAuNPs revealed excellent reversible, light-responsive aggregation and dispersion. Since heterocyclic azo-compounds such as AAPs are rather unknown so far but the research on molecular switches and light-responsive systems is recently very popular, our findings offer great potential to improve existing and to develop new supramolecular materials.

ASSOCIATED CONTENT

Supporting Information

The Supporting Information is available free of charge on the ACS Publications website at DOI: 10.1021/jacs.6b00484.

Experimental details including synthesis and further experimental data (PDF)

AUTHOR INFORMATION

Corresponding Author

*b.j.ravoo@uni-muenster.de

Notes

The authors declare no competing financial interest.

ACKNOWLEDGMENTS

This work was funded by the Volkswagen Foundation and the Deutsche Forschungsgemeinschaft (SFB 858). We thank Prof. Jens Voskuhl for supplying the perthiolated β-cyclodextrin. Julian Simke is acknowledged for the synthesis of the reference azobenzene.

REFERENCES

(1) Bandara, H. M. D.; Burdette, S. C. *Chem. Soc. Rev.* **2012**, *41*, 1809.
(2) Yagai, S.; Karatsu, T.; Kitamura, A. *Chem. - Eur. J.* **2005**, *11*, 4054.
(3) Beharry, A. A.; Wong, L.; Tropepe, V.; Woolley, G. A. *Angew. Chem., Int. Ed.* **2011**, *50*, 1325.
(4) Schrader, T. E.; Schreier, W. J.; Cordes, T.; Koller, F. O.; Babitzki, G.; Denschlag, R.; Renner, C.; Loweneck, M.; Dong, S.-L.; Moroder, L.; Tavan, P.; Zinth, W. *Proc. Natl. Acad. Sci. U. S. A.* **2007**, *104*, 15729.
(5) Schierling, B.; Noel, A.-J.; Wende, W.; Hien, L. T.; Volkov, E.; Kubareva, E.; Oretskaya, T.; Kokkinidis, M.; Roempp, A.; Spengler, B.; Pingoud, A. *Proc. Natl. Acad. Sci. U. S. A.* **2010**, *107*, 1361.
(6) Han, M.; Ishikawa, D.; Honda, T.; Ito, E.; Hara, M. *Chem. Commun.* **2010**, *46*, 3598.
(7) Siewierski, L. M.; Brittain, W. J.; Petrash, S.; Foster, M. D. *Langmuir* **1996**, *12*, 5838.
(8) Dietrich, P.; Michalik, F.; Schmidt, R.; Gahl, C.; Mao, G.; Breusing, M.; Raschke, M. B.; Priewisch, B.; Elsaesser, T.; Mendelsohn, R.; Weinelt, M.; Rueck-Braun, K. *Appl. Phys. A: Mater. Sci. Process.* **2008**, *93*, 285.
(9) Min, M.; Bang, G. S.; Lee, H.; Yu, B.-C. *Chem. Commun.* **2010**, *46*, 5232.
(10) Lee, J.-W.; Klajn, R. *Chem. Commun.* **2015**, *51*, 2036.
(11) Manna, D.; Udayabhaskararao, T.; Zhao, H.; Klajn, R. *Angew. Chem., Int. Ed.* **2015**, *54*, 12394.
(12) Köhntopp, A.; Dabrowski, A.; Malicki, M.; Temps, F. *Chem. Commun.* **2014**, *50*, 10105.
(13) Iamsaard, S.; Aßhoff, S. J.; Matt, B.; Kudernac, T.; Cornelissen, J. J. L. M.; Fletcher, S. P.; Katsonis, N. *Nat. Chem.* **2014**, *6*, 229.
(14) Bushuyev, O. S.; Tomberg, A.; Friščić, T.; Barrett, C. J. *J. Am. Chem. Soc.* **2013**, *135*, 12556.
(15) Ueno, A.; Yoshimura, H.; Saka, R.; Osa, T. *J. Am. Chem. Soc.* **1979**, *101*, 2779.
(16) Tomatsu, I.; Hashidzume, A.; Harada, A. *Macromolecules* **2005**, *38*, 5223.
(17) Zhao, Y. L.; Stoddart, J. F. *Langmuir* **2009**, *25*, 8442.
(18) Wang, D.; Wagner, M.; Butt, H.-J.; Wu, S. *Soft Matter* **2015**, *11*, 7656.
(19) Klajn, R. *Pure Appl. Chem.* **2010**, *82*, 2247.
(20) Voskuhl, J.; Sankaran, S.; Jonkheijm, P. *Chem. Commun.* **2014**, *50*, 15144.
(21) Ferris, D. P.; Zhao, Y.-L.; Khashab, N. M.; Khatib, H. A.; Stoddart, J. F.; Zink, J. I. *J. Am. Chem. Soc.* **2009**, *131*, 1686.
(22) Peng, L.; You, M.; Wu, C.; Han, D.; Öçsoy, I.; Chen, T.; Chen, Z.; Tan, W. *ACS Nano* **2014**, *8*, 2555.
(23) Fritz, E.-C.; Nimphius, C.; Goez, A.; Würtz, S.; Peterlechner, M.; Neugebauer, J.; Glorius, F.; Ravoo, B. J. *Chem. - Eur. J.* **2015**, *21*, 4541.
(24) Klajn, R.; Stoddart, J. F.; Grzybowski, B. A. *Chem. Soc. Rev.* **2010**, *39*, 2203.
(25) Liu, Z.; Jiang, M. *J. Mater. Chem.* **2007**, *17*, 4249.
(26) Ghosh, S. K.; Pal, T. *Chem. Rev.* **2007**, *107*, 4797.
(27) Saha, K.; Agasti, S. S.; Kim, C.; Li, X.; Rotello, V. M. *Chem. Rev.* **2012**, *112*, 2739.
(28) Nalluri, S. K. M.; Ravoo, B. J. *Angew. Chem., Int. Ed.* **2010**, *49*, 5371.
(29) Samanta, A.; Stuart, M. C. A.; Ravoo, B. J. *J. Am. Chem. Soc.* **2012**, *134*, 19909.
(30) Schenkel, J. H.; Samanta, A.; Ravoo, B. J. *Adv. Mater.* **2014**, *26*, 1076.
(31) *Molecular Switches*, 2nd ed.; Feringa, B., Browne, W. R., Eds.; Wiley-VCH: Weinheim, 2011.
(32) Yang, Y.; Hughes, R. P.; Aprahamian, I. *J. Am. Chem. Soc.* **2012**, *134*, 15221.
(33) Browne, W. R.; Feringa, B. L. *Nat. Nanotechnol.* **2006**, *1*, 25.
(34) Tian, H.; Yang, S. *Chem. Soc. Rev.* **2004**, *33*, 85.
(35) Nalluri, S. K. M.; Voskuhl, J.; Bultema, J. B.; Boekema, E. J.; Ravoo, B. J. *Angew. Chem., Int. Ed.* **2011**, *50*, 9747.

DOI: 10.1021/jacs.6b00484
J. Am. Chem. Soc. 2016, 138, 4547−4554

(36) Moratz, J.; Samanta, A.; Voskuhl, J.; Nalluri, S. K. M.; Ravoo, B. J. *Chem. - Eur. J.* **2015**, *21*, 3271.
(37) Roling, O.; Stricker, L.; Voskuhl, J.; Lamping, S.; Ravoo, B. J. *Chem. Commun.* **2016**, *52*, 1964−1966.
(38) For a review, see: Dong, M.; Babalhavaeji, A.; Samanta, S.; Beharry, A. A.; Woolley, G. A. *Acc. Chem. Res.* **2015**, *48*, 2662.
(39) Knie, C.; Utecht, M.; Zhao, F.; Kulla, H.; Kovalenko, S.; Brouwer, A. M.; Saalfrank, P.; Hecht, S.; Bléger, D. *Chem. - Eur. J.* **2014**, *20*, 16492.
(40) Siewertsen, R.; Neumann, H.; Buchheim-Stehn, B.; Herges, R.; Näther, C.; Renth, F.; Temps, F. *J. Am. Chem. Soc.* **2009**, *131*, 15594.
(41) Bléger, D.; Schwarz, J.; Brouwer, A. M.; Hecht, S. *J. Am. Chem. Soc.* **2012**, *134*, 20597.
(42) Samanta, S.; Beharry, A. A.; Sadovski, O.; McCormick, T. M.; Babalhavaeji, A.; Tropepe, V.; Woolley, G. A. *J. Am. Chem. Soc.* **2013**, *135*, 9777.
(43) Samanta, S.; McCormick, T. M.; Schmidt, S. K.; Seferos, D. S.; Woolley, G. A. *Chem. Commun.* **2013**, *49*, 10314.
(44) Weston, C. E.; Richardson, R. D.; Haycock, P. R.; White, A. J. P.; Fuchter, M. J. *J. Am. Chem. Soc.* **2014**, *136*, 11878.
(45) Zhang, L.; Zhang, H.; Gao, F.; Peng, H.; Ruan, Y.; Xu, Y.; Weng, W. *RSC Adv.* **2015**, *5*, 12007.
(46) Falvey, P.; Lim, C. W.; Darcy, R.; Revermann, T.; Karst, U.; Giesbers, M.; Marcelis, A. T. M.; Lazar, A.; Coleman, A. W.; Reinhoudt, D. N.; Ravoo, B. J. *Chem. - Eur. J.* **2005**, *11*, 1171.
(47) Rekharsky, M. V.; Inoue, Y. *Chem. Rev.* **1998**, *98*, 1875.
(48) Becker, M. M.; Ravoo, B. J. *Chem. Commun.* **2010**, *46*, 4369.
(49) Samanta, A.; Ravoo, B. J. *Chem. - Eur. J.* **2014**, *20*, 4966−4973.

DOI: 10.1021/jacs.6b00484
J. Am. Chem. Soc. 2016, 138, 4547−4554